# Cambridge Centre for Computational Chemical Engineering


## University of Cambridge

Department of Chemical Engineering



Preprint ISSN 1473 – 4273


# A Detailed Kinetic model for Combustion Synthesis of Titania from $TiCl_4$


Richard H. West [1] Raphael A. Shirley [1] Markus Kraft [1]

C. Franklin Goldsmith [2] William H. Green [2]



released: 24 January 2008



[1] Department of Chemical Engineering
University of Cambridge
New Museums Site
Pembroke Street
Cambridge, CB2 3RA
UK
E-mail: mk306@cam.ac.uk

[2] Massachusetts Institute of Technology
77 Massachusetts Avenue
Cambridge MA 02139
USA



Preprint No. 55


**c4e**


*Key words and phrases:* titanium dioxide, kinetic model, chemical mechanism, population balance, titanium tetrachloride

**Edited by**
Cambridge Centre for Computational Chemical Engineering
Department of Chemical Engineering
University of Cambridge
Cambridge CB2 3RA
United Kingdom.

**Fax:** + 44 (0)1223 334796
**E-Mail:** c4e@cheng.cam.ac.uk
**World Wide Web:** http://www.cheng.cam.ac.uk/c4e/

**Abstract**

The combustion of $TiCl_4$ to synthesize $TiO_2$ nanoparticles is a multimillion tonne per year industrial process, the fundamental details of which are still not known. The gas-phase kinetic model presented by West et al. (*Ind. Eng. Chem. Res.* **46** (19), 2007, 6147–6156) is improved upon using Density Functional Theory (DFT) and Variational Transition State Theory (VTST) calculations. The pressure-dependent rate expression for the reaction $TiCl_3$ + $O_2$ $\rightleftharpoons$ $TiO_2Cl_3$ is found using VTST, a stable $Ti_2O_2Cl_6$ species is located on the minimum energy pathway for $TiCl_3 + TiO_2Cl_3 \leftrightharpoons 2\ TiOCl_3$, and a number of new elementary reactions are added. Thermochemical data are provided for $Ti_2O_2Cl_6$, $Ti_2O_2Cl_5$ and $TiCl_2OCl$. The new kinetic model is used to simulate a rapid compression machine (RCM) and a plug flow reactor (PFR) described in the literature. Agreement with the RCM measurements is good, but simulations of the PFR are less satisfying, suggesting that surface deposition on the reactor walls may have dominated these measurements, which have been the basis of many theoretical models. Finally, the gas-phase kinetic model is coupled to a particle population balance model (PBM) incorporating inception, coagulation, growth, and sintering, to investigate the influence of PFR temperature on particle size distributions. The extension of the PBM to track primary particles allows creation of TEM-style images from the simulation and first results are presented.

# Contents

# 1 Introduction

Titanium dioxide ($TiO_2$) is widely used as a pigment, as a catalyst support, and as a photocatalyst. The combustion of titanium tetrachloride ($TiCl_4$) to synthesize $TiO_2$ nanoparticles is a multi-million tonne per year industrial process [6]. In this "chloride" process, purified titanium tetrachloride is oxidised at high temperatures (1500–2000 K) in a pure oxygen plasma or flame to produce $TiO_2$ particles [4, 10]. This paper builds on the work detailed in [32], which provides a full introduction to this field.

There have been a few experimental investigations of the kinetics of the system; in the most frequently cited study, Pratsinis et al. [25] reported the overall oxidation kinetics of $TiCl_4$ at 973–1273 K determined by measuring the concentration of unreacted $TiCl_4$ leaving a plug flow reactor (PFR). The rate was found to be first order with respect to $TiCl_4$ and largely independent of $O_2$ concentration, with a rate coefficient

$$k = 8.26 \times 10^4 \text{ s}^{-1} \exp\left(\frac{-88.8 \text{ kJ/mol}}{RT}\right) \tag{1}$$

where $T$ is the temperature and $R$ is the molar gas constant.

This experimental work has been the basis for many theoretical studies of $TiO_2$ nanoparticle dynamics [18, 29, 31**?** ]. However, these experiments were performed at temperatures and pressures much lower than those used in the industrial process. Extrapolation of kinetic data to this degree must be treated with caution.

Attempts have also been made to measure the kinetics in a rapid compression machine (RCM), allowing higher temperatures and pressures to be reached for short times [26].

Recently a framework for a comprehensive model that attempts to describe the phenomena at different scales has been developed [33]. Ab-initio and density functional theory (DFT) investigations [32] provided the thermochemical data needed for the first thermodynamically consistent detailed kinetic model of the gas phase combustion of $TiCl_4$. Previous models greatly simplify the chemical processes to a single step and are unable to capture the details of temperature and concentration dependencies. Coupled to this detailed chemistry was a new population balance model, solved using a stochastic technique, that extended previous surface-volume models to track primary particles within each agglomerate in the population.

The mechanism for surface growth of $TiO_2$ (deposition from the gas phase) is the subject of both experimental [28] and computational [14, 33] studies. Although progress is being made towards a better understanding of the surface chemistry of this system, due to a lack of detailed kinetic data, current population balance models [24, 29, 31, 33**?** ], like this work, rely on the simple first-order rate expression measured by Ghoshtagore at 673–1020 K [8]:

$$\frac{dN_{\text{TiO}_2}}{dt} = A[\text{TiCl}_4] 4.9 \times 10^3 \text{ cm s}^{-1} \times \exp\left(\frac{-74.8 \text{ kJ mol}^{-1}}{RT}\right) \tag{2}$$

where $N_{\text{TiO}_2}$ is the amount of $TiO_2$ deposited, $A$ is the surface area, and $[TiCl_4]$ is the concentration of $TiCl_4$ in the gas phase.

The purpose of this paper is (i) to improve the current detailed chemical model by identifying new species and reactions and providing thermodynamic and kinetic data; (ii) to validate the mechanism by comparing it to experiments performed in an RCM; and (iii) to simulate the PFR that led to the widely-used overall reaction rate expression, investigating the possible effect of wall deposition and the influence of temperature on particle size distributions.

# 2 Reaction Mechanism

The starting point for our reaction mechanism is the kinetic model detailed in West et al. [33]. This model includes 51 reactions, most of them with only rough estimates of their rates. The potential energy surfaces (PESs) for several reactions were investigated using the DFT package DMol$^3$. We focus here on two reactions. First

$$\mathrm{TiCl_3 + O_2 \leftrightharpoons TiO_2Cl_3} \tag{R1}$$

(R19 in [33]) because a flux analysis revealed it lies on the main reaction pathway, and it is likely to be greatly slowed by falloff. Second

$$\mathrm{TiCl_3 + TiO_2Cl_3 \leftrightharpoons 2\ TiOCl_3}$$

(R21 in [33]), because a sensitivity analysis found the overall reaction rate to be most sensitive to the rate of this elementary reaction.

## 2.1 Reaction $\mathrm{TiCl_3 + O_2 \leftrightharpoons TiO_2Cl_3}$

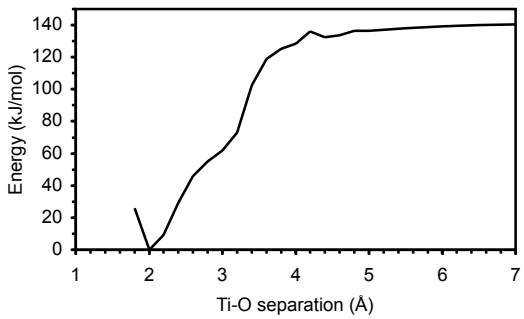


**Figure 1:** *Minimum energy pathway for reaction R1 calculated with HCTH density functional in DMol$^3$.*

Reaction R1 is barrierless and the rate of stabilization of $\mathrm{TiCl_3O_2}$ is pressure dependent. Quantum-chemical calculations were repeated using the CBS-QB3 [20] compound method in Gaussian03 [7]. The CBS-QB3 energies were calculated for the reactants and product. The B3LYP/6-311G(2d,d,p) Ti–O bond length was $R_e$ = 1.99 Å. For the transition state minimum energy path (MEP), constrained optimizations were performed at

fixed Ti–O bond lengths of $R$ = 2.5, 3.0, 3.5, 4.0, 4.5, and 5.0 Å., followed by CBS-QB3 calculations. The pressure-dependent reaction rate was calculated using a RRKM/Master Equation code, VariFlex [16]. The method used to calculate the variational transition state theory rate constant is similar to the method described in [30], in which a rigid-rotor harmonic-oscillator approximation is made for each step in the MEP. For both the stabilized product and the six fixed points on the MEP, the ClTi–OO torsional frequency was treated as a free rotor. Additional anharmonic effects may be present – e.g. the umbrella modes in $TiCl_3O_2$ and the MEP with frequencies below 200 $cm^{-1}$ – but were not included in the calculations. Variflex calculations were performed at pressures between 0.001 and 30 bar, and temperatures between 400 and 2000 K. The resulting $k(T, p)$ matrix was fit to a standard Lindemann [19] equation with a Troe broadening parameter [9] for use in Chemkin [15] and Cantera [11]; these parameters are given in Table 1.

## 2.2 Reaction $TiCl_3$ + $TiO_2Cl_3 \leftrightharpoons$ 2 $TiOCl_3$

When investigating the PES for the exothermic reaction $TiCl_3 + TiO_2Cl_3 \leftrightharpoons 2\ TiOCl_3$, the intermediate $Ti_2O_2Cl_6$ was found to be stable (a minimum on the PES), with an electronic energy 225 kJ/mol below the products. The reaction was split into two elementary reactions.

$$TiO_2Cl_3 + TiCl_3 \leftrightharpoons Ti_2O_2Cl_6 \quad \text{(R2)}$$

$$2\ TiOCl_3 \leftrightharpoons Ti_2O_2Cl_6 \quad \text{(R3)}$$

The minimum energy pathway (MEP) for R2 was found to be barrierless at this level of theory, and no transition state (saddle point on the PES) could be found for R3, although as the distance between the Ti atoms is increased, the minimum energy pathway on the electronic potential energy surface leads to a $TiCl_3$-O-O structure with a dangling oxygen, which is higher in energy than the $TiO_2Cl_3$ structure reported in [32], which has both O atoms close to the Ti.

Following the addition of $Ti_2O_2Cl_6$ to the kinetic model, a number of additional reactions were added. The abstraction of one Cl by either Cl or $TiCl_3$ radicals leads to $Ti_2O_2Cl_5$, another new species; further Cl abstraction leads to $Ti_2O_2Cl_4$, a species already in the kinetic model. These four reactions were added to the model (R4–R7).

## 2.3 Additional reactions

In addition to the four reactions described above, some additional reactions were added to the kinetic model, including reactions of the species $TiCl_2OCl$ which had not previously been considered. See Tab. 1 for all the new reactions.

The rate expression for R16 was taken from DeMore et al. [5], and that for R17 was found by fitting a modified Arrhenius expression to all the data in the NIST kinetics database [21]. The remaining rate parameters were estimated as having a pre-exponential factor, $A$, given by the collision limit $1 \times 10^{13}$ $cm^3$ $mol^{-1}$ $s^{-1}$, and the activation energy, $E_a$, in the exothermic direction was taken to be zero.

**Table 1:** *Reaction mechanism equations*

| No | Reaction | $\Delta H^\circ_{298K}$ [a] | $A$ [b] | $n$ | $E_a$ [a] | Ref. |
|---|---|---|---|---|---|---|
| R1 | $P_\infty$: $TiCl_3 + O_2 \rightleftharpoons TiO_2Cl_3$ | −277 | $1.925\times10^{35}$ | −6.577 | 41384 | |
| | $P_0$: $TiCl_3 + O_2 + M \rightleftharpoons TiO_2Cl_3 + M$ | | $1.060\times10^{36}$ [c] | −6.319 | 0 | |
| | Troe parameters: $\alpha = 0.1183$, $T^{***} = 26.93$ K, $T^* = 10^5$ K, $T^{**} = 5219.3$ K | | | | | |
| Removed from mechanism | | | | | | |
| | $TiCl_3 + TiO_2Cl_3 \rightleftharpoons 2\ TiOCl_3$ | −7 | $1.00\times10^{13}$ | 0 | 0 | |
| Replacements | | | | | | |
| R2 | $TiO_2Cl_3 + TiCl_3 \rightleftharpoons Ti_2O_2Cl_6$ | −232 | $1.00\times10^{13}$ | 0 | 0 | |
| R3 | $2\ TiOCl_3 \rightleftharpoons Ti_2O_2Cl_6$ | −225 | $1.00\times10^{13}$ | 0 | 0 | |
| Additional reactions | | | | | | |
| R4 | $Cl_2 + Ti_2O_2Cl_5 \rightleftharpoons Cl + Ti_2O_2Cl_6$ | −110 | $1.00\times10^{13}$ | 0 | 0 | |
| R5 | $Cl + Ti_2O_2Cl_5 \rightleftharpoons Cl_2 + Ti_2O_2Cl_4$ | −401 | $1.00\times10^{13}$ | 0 | 0 | |
| R6 | $TiCl_3 + Ti_2O_2Cl_5 \rightleftharpoons TiCl_4 + Ti_2O_2Cl_4$ | −546 | $1.00\times10^{13}$ | 0 | 0 | |
| R7 | $TiCl_3 + Ti_2O_2Cl_6 \rightleftharpoons TiCl_4 + Ti_2O_2Cl_5$ | −35 | $1.00\times10^{13}$ | 0 | 0 | |
| R8 | $TiCl_2OCl \rightleftharpoons TiOCl_2 + Cl$ | −2 | $1.00\times10^{13}$ | 0 | 0 | |
| R9 | $TiCl_2OCl + Cl \rightleftharpoons TiCl_3 + ClO$ | −42 | $1.00\times10^{13}$ | 0 | 0 | |
| R10 | $TiCl_2OCl + Cl \rightleftharpoons TiOCl_3 + Cl$ | −164 | $1.00\times10^{13}$ | 0 | 0 | |
| R11 | $TiCl_2OCl + Cl \rightleftharpoons Cl_2 + TiOCl_2$ | −244 | $1.00\times10^{13}$ | 0 | 0 | |
| R12 | $TiCl_3 + ClOO \rightleftharpoons TiCl_4 + O_2$ | −363 | $1.00\times10^{13}$ | 0 | 0 | |
| R13 | $TiCl_4 + O_3 \rightleftharpoons TiCl_3 + ClO + O_2$ | 226 | $1.00\times10^{13}$ | 0 | 226 | |
| R14 | $TiOCl_3 + O_3 \rightleftharpoons TiO_2Cl_3 + O_2$ | −277 | $1.00\times10^{13}$ | 0 | 0 | |
| R15 | $TiO_2Cl_2 + ClOO \rightleftharpoons TiO_2Cl_3 + O_2$ | −314 | $1.00\times10^{13}$ | 0 | 0 | |
| R16 | $ClOO + Cl \rightleftharpoons Cl_2 + O_2$ | −219 | $1.39\times10^{14}$ | 0 | 0 | [5] |
| R17 | $O_3 + O \rightleftharpoons 2\ O_2$ | −391 | $5.47\times10^{12}$ | 0.00322 | 17.4 | [21] |

[a] kJ mol$^{-1}$ [b] cm$^3$ mol$^{-1}$ s$^{-1}$ [c] cm$^6$ mol$^{-2}$ s$^{-1}$

## 2.4 Thermochemistry

For species added to the kinetic model in this work, thermochemical data were calculated using the same method described in [32]. Molecular geometries (Fig. 2) were optimized and analytical harmonic frequencies calculated in Gaussian 03 [7] using the B97-1 density functional [13], as recommended by Boese *et al.* [2]. The basis set was 6-311+G(d,p), a supplemented, triple-zeta basis set that should be large enough to ensure that the basis set truncation error is comparable with, or smaller than, the inherent errors in the DFT [2].

To establish the spin multiplicity of the ground state, the lowest-energy state of different spin multiplicity was also calculated. $Ti_2O_2Cl_6$ is a singlet in its ground state; $TiCl_2OCl$ and $Ti_2O_2Cl_5$ are doublets.

Isogyric reaction schemes are desired to link the calculated species to reference species with well-known enthalpies of formation. The choice is especially important, as explained in [32].

The standard enthalpy of formation of $Ti_2O_2Cl_6$ was derived from the isogyric reaction $Ti_2O_2Cl_6 \rightleftharpoons 2\ TiOCl_2 + Cl_2$ and $Ti_2O_2Cl_5$ from $Ti_2O_2Cl_5 + TiCl_4 \rightleftharpoons 2\ TiOCl_2 + Cl_2 + TiCl_3$. $TiCl_2OCl$ was derived from the anisogyric reaction $TiCl_2OCl \rightleftharpoons TiOCl_2 + Cl$ so is expected to be the least accurately determined $\Delta_f H^\circ_{298\,K}$.

Heat capacities ($C_p$), integrated heat capacites ($H(T) - H(0\ \mathrm{K})$) and entropies ($S$) were calculated for temperatures in the range 100–3000 K using the rigid-rotator harmonic-

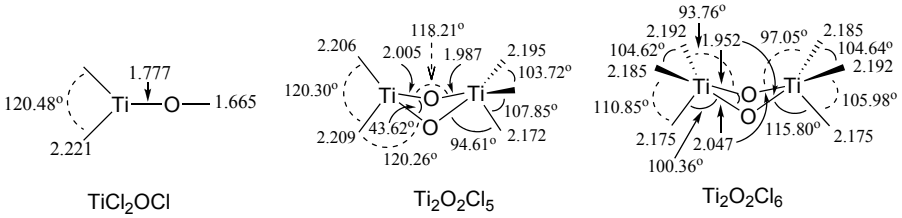


**Figure 2:** *Molecular structures of* $\mathrm{TiCl_2OCl}$, $\mathrm{Ti_2O_2Cl_5}$ *and* $\mathrm{Ti_2O_2Cl_6}$. *Bond lengths are in Ångströms, and unlabelled atoms are chlorine.*

oscillator (RRHO) approximation, taking unscaled vibrational frequencies and rotational constants from the B97-1 calculations (see Tab. 2). Polynomials in the NASA form [12] for use in Chemkin and Cantera were fitted to $C_\mathrm{p}(T)/R$, $H^\circ$ and $S^\circ$ over the temperature ranges 100 K–$T_c$ and $T_c$–3000 K, constrained to ensure $C_p(T)$ and its first two derivatives matched at the common temperature $T_c$, which was varied to optimise the overall fit for each species.

**Table 2:** *Calculated thermochemistry at 298 K.*

| species | $\Delta_f H^\circ_{298\,K}$ kJ/mol | $S^\circ_{298\,K}$ J/mol K | rot. const. GHz | vibrational frequencies $\mathrm{cm}^{-1}$ |
|---|---|---|---|---|
| $\mathrm{TiCl_2OCl}$ | $-475$ | 396.9 | 1.9445, 0.9729, 0.6484 | 17.1, 44.8, 93.7, 131, 174, 341, 474, 483, 950 |
| $\mathrm{Ti_2O_2Cl_6}$ | $-1503$ | 562.3 | 0.5965, 0.2506, 0.2497 | 17.9, 18.7, 36.3, 84.8, 93.6, 101, 115, 135, 135, 137, 155, 163, 206, 299, 324, 388, 404, 455, 473, 487, 505, 509, 574, 902 |
| $\mathrm{Ti_2O_2Cl_5}$ | $-1272$ | 537.5 | 0.7562, 0.2939, 0.2611 | 14.1, 28.3, 45.8, 79.5, 82.3, 100, 118, 130, 140, 162, 194, 318, 335, 366, 401, 473, 483, 493, 501, 575, 885 |

# 3 Population Balance Modelling

To simulate the comprehensive model of chemistry and particle dynamics, we use the extended surface-volume model with primary particle tracking described in [23, 33], coupled to the gas phase chemistry simulation using operator splitting [3]. Numerical validation of this population balance solver is provided in [3, 22].

An agglomerate particle in the population balance is described by the number of $\mathrm{TiO_2}$ monomers in the particle, $M$, the surface area of the particle, $A$, and the number of $\mathrm{TiO_2}$ monomers in each of the primary particles that make up the agglomerate, $(m_1, m_2, m_3, \ldots)$. All other particle properties, and hence particle process rates, are calculated from $M$ and $A$. The stochastic particle method [22] used here to solve the population balance makes it computationally cheap to track many internal co-ordinates within the population.

In the current study, the collision of any two molecules containing two or more Ti atoms each is treated as a particle inception. The rate of these events is dependent on the con-

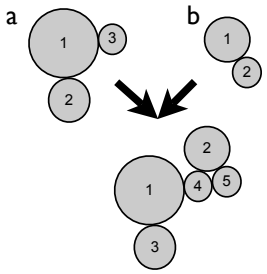


**Figure 3:** *Coagulation of particles $a$ and $b$.*

centration of the species involved, and is estimated according to collision theory. When a particle is first incepted from the gas phase, it is assumed to be spherical, and to contain one primary particle.

The rate of particle growth due to surface reactions with the gas phase was calculated using the first order expression from [8] (Eq. 2). The change in particle surface area due to surface growth is determined according to [23]. Mass added to a particle through surface growth is distributed amongst the constituent primary particles randomly, with probabilities proportional to their spherical surface areas.

The rates of collisions between particles of different sizes and shapes is determined by the coagulation kernel, in this case a function of $M$ and $A$. Different coagulation kernels are appropriate in different conditions (particle size and gas pressure); see [27] for details. These coagulation kernels are also used to model the particle inception processes.

When two particles coagulate the monomer count and surface area are conserved, and the lists of constituent primary particles are appended to one another. For example, when two particles $a$ and $b$, with properties $(M_a, A_a, m_{a1}, m_{a2}, m_{a3})$ and $(M_b, A_b, m_{b1}, m_{b2})$, coagulate as illustrated in Fig. 3, the resulting agglomerate particle will be given by $(M_a + M_b, A_a + A_b, m_{a1}, m_{b1}, m_{a2}, m_{a3}, m_{b2})$.

Sintering is modelled following the approach of Xiong and Pratsinis [34], by assuming that the excess agglomerate surface area, over that of a spherical particle with the same mass, decays exponentially with a characteristic time taken from Kobata et al. [17].

The surface area of an aggregate particle in this simulation is tracked independently and determined by the sintering and surface growth models. The list of primary particles is updated to match this surface area value according to a scheme, inspired by Ostwald ripening, that involves removing small primary particles from the list and redistributing their mass over the larger ones. For this purpose primary particles are assumed to be spherical with the same density as bulk rutile.

In order to generate shape information, to aid visualisation of the particles, the positions of the primary particles within a particle are generated in a post-processing step.

# 4 Simulations

## 4.1 Rapid Compression Machine

The PhD thesis by Raghavan describes investigations of the kinetics of $TiCl_4$ oxidation using a rapid compression machine (RCM) [26]. A mixture of 0.3 mol% $TiCl_4$ and 1 mol% $O_2$ in Argon was loaded into a cylinder at reduced pressure, then rapidly compressed causing temperature and pressure of the gas to rise quickly. The temperature was calculated from the pressure, volume, and starting temperature, according to a hot-core model in which 20% of the volume (near the walls) is compressed isothermally. The piston was designed to bounce, resulting in a short peak in temperature, found to be well approximated by a lorentzian. The reaction time reported was the half-width at half-maximum (HWHM) of a lorentzian fitted to the top 10% of the temperature profile. The concentration of $TiCl_4$ was measured before and after compression using FTIR spectroscopy.

This RCM was simulated here with the new gas-phase kinetic model, using Cantera and Python. In our simulation, the piston was driven sinusoidally for one stroke, with a speed and compression ratio adjusted to ensure that a Lorentzian least-squares fitted to the hottest 10% or our temperature profile had a $T_p$ and HWHM equal to Raghavan's reported values. This was repeated for the sixteen combinations of $T_p$ and $t_c$ reported in [26]. The shape of the temperature profile from this sinusoidal compression is similar to the temperature profiles of the RCM given in Raghavan [26]. The simulation was spatially homogeneous, so following the hot-core description in Raghavan [26], the simulated conversion was scaled by 0.8 (20% of the gas remained unreacted). Because the gas is heated rapidly and for a short time the walls do not heat up, so surface reactions were neglected.

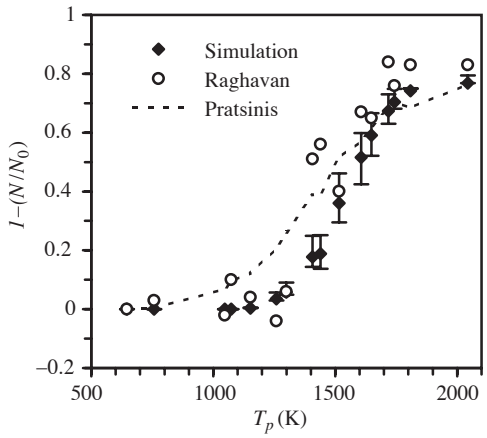


**Figure 4:** *Fraction of $TiCl_4$ consumed after rapid compression in the RCM, plotted against the peak temperature reached. The lower limit shows a simulation with $t_c$=10 ms, the upper limit 40 ms, and the filled diamond the $t_c$ that was reported for the corresponding measurement (white circle) from Raghavan [26]*

Figure 4 shows the fraction of $TiCl_4$ consumed ($1 - N/N_0$) plotted against the peak tem-

perature reached in the reactor ($T_p$) from Raghavan's thesis [26] with our simulation results superimposed. The design of the RCM meant that the peak temperature $T_p$ and the reaction time $t_c$ could not be controlled independently (a higher $T_p$ usually meant a shorter $t_c$). The extent of reaction obviously depends on the reaction time, so simply plotting $(1 - N/N_0)$ as a function of $T_p$ without mentioning $t_c$ is misleading. The bars on the simulation results in Fig. 4 indicate the sensitivity with respect to compression time $t_c$: the lower limit is the result of $t_c$=10 ms, the upper limit is 40 ms, and the central mark is the $t_c$ that was reported for the corresponding $N/N_0$ measurement in [26]. Also shown (dashed line) are the results of simulations using the one-step Arrhenius rate expression (1) from [25].

The kinetic model agrees reasonably well with the experiments without any fitting of parameters. The fraction of $TiCl_4$ consumed during compression to a given temperature is somewhat lower in our simulations than the reported measurements, but, although no error bars were reported for the measurements, we expect the uncertainties in the temperature estimations to be significant (see discussion).

## 4.2 Plug Flow Reactor (PFR)

The combined simulation coupling the gas phase kinetic model to the particle dynamics model was used to simulate the tubular flow reactor used by Pratsinis [25] to measure the overall reaction kinetics. In Pratsinis et al. [25], a flow of 0.2 mol% $TiCl_4$ and 1 mol% $O_2$ in Argon was fed to a 3.18 mm-I.D. tube, a ∼30 cm section of which was heated to 973–1273 K in a furnace. The concentration of $TiCl_4$ leaving the flow tube ($C_o$) was measured using FTIR spectroscopy. Assuming that the reaction rate is first order in [$TiCl_4$] with Arrhenius kinetics ($k_{\text{eff}} = A \exp(-E_a/RT)$) and that all reaction occurs during the time $t$ that the gas spends in an isothermal zone at temperature $T$ then

$$-\big(\ln(C_o/C_i)\big)/t\big) = k_{\text{eff}} = A \exp(-E_a/RT). \tag{3}$$

A plot of $\ln\big(-\big(\ln(C_o/C_i)\big)/t\big)$ versus $1/T$ (Fig. 5) would thus give a straight line from which the apparent activation energy $E_a$ and pre-exponential constant $A$ can be determined. This is the analysis performed in Pratsinis et al. [25], and our simulation results are processed the same way for easy comparison. The assumption of constant $T$ for a time $t$ was only made for the analysis: the simulations covered the entire temperature profile (given in Pratsinis et al. [25]) and included thermal expansion of the gas as the temperature varied.

The simulations using our new gas-phase kinetic model (Fig. 5, solid lines) consume much less $TiCl_4$ than the observations reported in Pratsinis et al. [25]. At 1133 K the $k_{\text{eff}}$ fitted to the simulation is between 14 and 45 times lower (slower rate) than that fitted to the experiment, depending on which residence time is simulated. The apparent activation energy is higher in the simulation, so at 993 K the discrepancy increases to $k_{\text{eff}}^{\text{expt}}/k_{\text{eff}}^{\text{sim}} = 5.2 \times 10^3$ in the worst case. Possible reasons for this discrepancy will be discussed in a later section.

The simulations were repeated allowing for deposition and reaction of $TiCl_4$ on the inside surface of the tube, using the expression for surface growth of a $TiO_2$ film given by

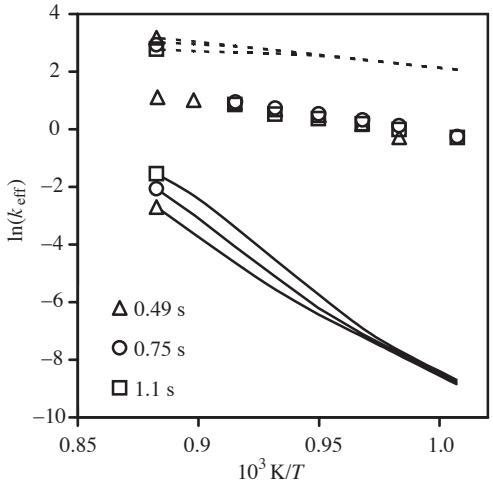


**Figure 5:** *Arrhenius plot of plug flow reactor at three different residence times. Unconnected points are measurements reported in [25], lines are our simulations: dotted with deposition on the reactor walls and solid without.*

Ghoshtagore [8] (Eqn. 2).

In these simulations (Fig. 5, dotted lines), 500 times as much $TiCl_4$ was consumed through reaction on the walls as through reactions in the gas phase, and the overall consumption of $TiCl_4$ was *higher* than that observed in Pratsinis et al. [25]. This may be partially because mass transport limitations were not modelled. Also, Ghoshtaghore's rate expression is for much higher $O_2$ partial pressures, so would be expected to over-predict wall reactions in the conditions modelled here.

### 4.3 Particle Properties

The flow tube reactor was simulated using the coupled population balance model. This allows access to a wealth of information far beyond the rate of consumption of $TiCl_4$. Figure 6 shows the size distribution of titania particles at the end of the simulation (40 cm downstream from the midpoint of the tube, when the temperature has returned to 298 K) and Fig. 7 shows TEM-style images of some of the particles.

As the temperature of the PFR is increased, so does the average size of the particles produced. This is the same as the trend observed by Akhtar et al. [1] in a similar PFR.

## 5 Discussion

A rapid compression machine seems to be a useful tool for measuring gas-phase kinetics at high temperatures and pressures, but at less expense than a shock-tube. However, uncertainties in the temperature measurements are likely to be significant. The peak tem-

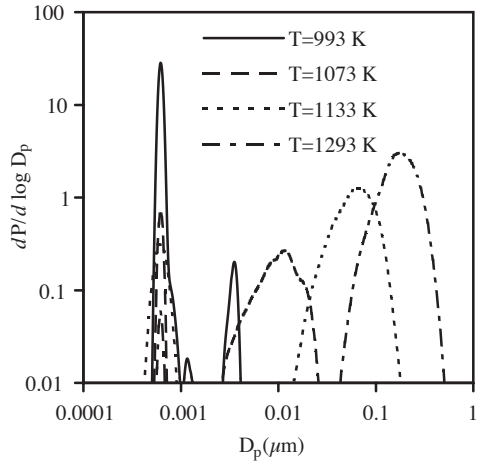


**Figure 6:** *Particle size distributions from the PFR simulation with residence time in the hot-zone of 0.49 s.*

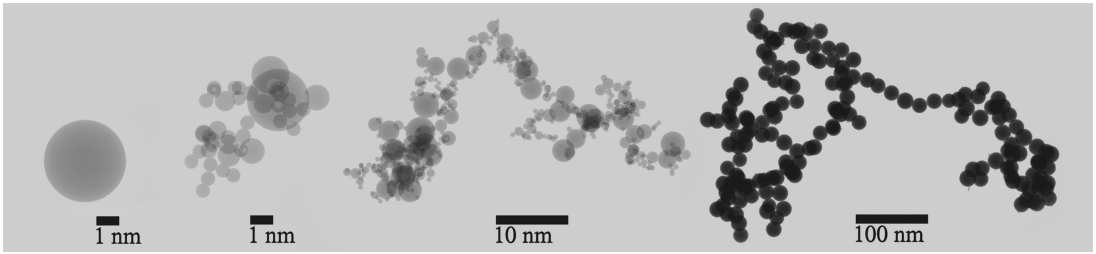


**Figure 7:** *Simulated TEM Images from the exit of the PFR simulation with residence time in the hot-zone of 0.49 s and furnace temperatures 993, 1017, 1073 and 1293 K (left to right).*

perature $T_p$ was deduced from measurements of pressure, volume, and the starting temperature $T_0$, giving three causes for concern. First, an error in measuring $T_0$ is amplified in $T_p$. Second, the deduced $T_p$ is very sensitive to errors in measuring the maximum piston displacement. Third, the assumptions necessary for this deduction are hard to verify. Unfortunately, Raghavan does not give estimates of the errors in $N/N_0$ or $T_p$ in Fig. 4, but we expect they are not small enough to justify adjusting parameters in our kinetic model to fit these experiments. The 20% dead-zone in the model ensures that no simulation will ever match the observations in which $(1 - N/N_0) > 0.8$, whichever kinetics are used.

Plug flow reactors are often used to measure rates, and the careful measurements in [25] seem like a useful check for any kinetic model of $TiCl_4$ oxidation. At first glance the disagreement of four orders of magnitude between the first-order rate fitted to the experiments and that fitted to the simulations suggests a problem with the new gas-phase kinetic model used in the simulations. Indeed, this may be the case. However, there is an alternative possibility.

Due to the small internal diameter of the tube, the surface-area to volume ratio is high, and including surface reaction on the tube wall has a large effect on the simulations. It is possible that the consumption of $TiCl_4$ being measured in the experiments was mostly happening on the walls of the tube. The rate expression derived from these measurements, however, has been widely used to simulate gas-phase reactions, and has often been used as an inception rate for $TiO_2$ particle population balance models. Yoon et al. [35] observed that, in their tubular reactor of diameter 2.7cm, up to 92% of $TiO_2$ production was on the walls. Further investigation of both gas and surface kinetics may be required to resolve this issue.

# 6 Conclusions

The first detailed gas-phase kinetic model for $TiCl_4$ oxidation [33] has been improved using DFT and VTST calculations, which have provided new thermochemical and kinetic data. This improved kinetic model is in agreement with the experimental data from a rapid compression machine [26], with the results of the model falling within the estimated uncertainties of the experimental measurements. Simulations of a plug flow reactor, however, suggest that surface reactions on the reactor walls may have dominated the experimental measurements [25]. Many models simulating $TiO_2$ formation from the gas phase have relied on rate expressions derived from these experimental measurements. The improved kinetic model thus represents an important advance in the understanding of $TiO_2$ particle formation.

Finally, the improved gas-phase kinetic model was coupled to a particle population balance model (PBM) to investigate the influence of PFR temperature on particle size distributions. The traditional surface-volume PBM was extended to track the growth and sintering of primary particles within each particle. This allowed creation of TEM-style images of the agglomerate particles from the simulation, which are presented herein.

# Acknowledgments

The authors would like to thank Prof. Stephen Klippenstein for help with the Variflex calculations, Tioxide Europe Limited (TEL) for the financial support of RAS, the EPSRC for grant number EP/E01724X/1, and both the EPSRC and TEL for the financial support of RHW through an Industrial CASE studentship.

# References


[1] M. K. Akhtar, Y. Xiong, and S. E. Pratsinis. Vapor synthesis of titania powder by titanium tetrachloride oxidation. *AIChE J.*, 37(10):1561–1570, 1991. doi:10.1002/aic.690371013.

[2] A. D. Boese, J. M. L. Martin, and N. C. Handy. The role of the basis set: Assessing density functional theory. *J. Chem. Phys.*, 119(6):3005–3014, Aug 2003. ISSN 0021-9606.

[3] M. Celnik, R. Patterson, M. Kraft, and W. Wagner. Coupling a stochastic soot population balance to gas-phase chemistry using operator splitting. *Combust. Flame*, 148 (3):158–176, 2007. doi:10.1016/j.combustflame.2006.10.007.

[4] J. C. Deberry, M. Robinson, M. Pomponi, A. J. Beach, Y. Xiong, and K. Akhtar. Controlled vapor phase oxidation of titanium tetrachloride to manufacture titanium dioxide, us patent 6387347. US Patent, 2002.

[5] W. DeMore, S. Sander, D. Golden, R. Hampson, M. Kurylo, C. Howard, A. Ravishankara, C. Kolb, and M. Molina. Chemical kinetics and photochemical data for use in stratospheric modeling, Evaluation Number 15. Technical Report JPL 06-2, NASA Jet Propulsion Laboratory, Jet Propulsion Laboratory, 4800 Oak Grove Drive, Pasadena, California 91109-8099 USA, 1997. URL `http://jpldataeval.jpl.nasa.gov/`.

[6] J. Emsley. *Molecules at an Exhibition*. Oxford University Press, 1999.

[7] M. J. Frisch, G. W. Trucks, H. B. Schlegel, G. E. Scuseria, M. A. Robb, J. R. Cheeseman, J. A. Montgomery, Jr., T. Vreven, K. N. Kudin, J. C. Burant, J. M. Millam, S. S. Iyengar, J. Tomasi, V. Barone, B. Mennucci, M. Cossi, G. Scalmani, N. Rega, G. A. Petersson, H. Nakatsuji, M. Hada, M. Ehara, K. Toyota, R. Fukuda, J. Hasegawa, M. Ishida, T. Nakajima, Y. Honda, O. Kitao, H. Nakai, M. Klene, X. Li, J. E. Knox, H. P. Hratchian, J. B. Cross, V. Bakken, C. Adamo, J. Jaramillo, R. Gomperts, R. E. Stratmann, O. Yazyev, A. J. Austin, R. Cammi, C. Pomelli, J. W. Ochterski, P. Y. Ayala, K. Morokuma, G. A. Voth, P. Salvador, J. J. Dannenberg, V. G. Zakrzewski, S. Dapprich, A. D. Daniels, M. C. Strain, O. Farkas, D. K. Malick, A. D. Rabuck, K. Raghavachari, J. B. Foresman, J. V. Ortiz, Q. Cui, A. G. Baboul, S. Clifford, J. Cioslowski, B. B. Stefanov, G. Liu, A. Liashenko, P. Piskorz, I. Komaromi, R. L. Martin, D. J. Fox, T. Keith, M. A. Al-Laham, C. Y. Peng, A. Nanayakkara, M. Challacombe, P. M. W. Gill, B. Johnson, W. Chen, M. W. Wong, C. Gonzalez, and J. A. Pople. Gaussian 03, Revision C.02, 2003. Gaussian, Inc., Wallingford, CT, 2004.

[8] R. N. Ghoshtagore. Mechanism of heterogeneous deposition of thin film rutile. *J. Electrochem. Soc.*, 117:529–534, 1970. doi:10.1149/1.2407561.

[9] R. Gilbert, K. Luther, and J. Troe. Theory of thermal unimolecular reactions in the fall-off range. ii. weak collision rate constants. *Ber. Bunsenges. Phys. Chem*, 87: 169–177, 1983.

[10] R. A. Gonzalez, C. D. Musick, and J. N. Tilton. Process for controlling agglomeration in the manufacture of $TiO_2$, us patent 5508015. US Patent, April 1996.

[11] D. G. Goodwin. An open source, extensible software suite for CVD process simulation. In M. Allendorff, F. Maury, and F. Teyssandier, editors, *Chemical Vapor Deposition XVI and EUROCVD 14*, volume 2003-08 of *ECS Proceedings*, pages 155–162, Pennington, New Jersey, USA, 2003. The Electrochemical Society, The Electrochemical Society. URL www.cantera.org.

[12] S. Gordon and B. J. McBride. Computer program for calculation of complex chemical equilibrium composition, rocket performance, incident and reflected shocks and chapman-jouguet detonations. Technical Report NASA-SP-273, NASA, 1976.

[13] F. A. Hamprecht, A. J. Cohen, D. J. Tozer, and N. C. Handy. Development and assessment of new exchange-correlation functionals. *J. Chem. Phys.*, 109(15):6264–6271, October 1998.

[14] O. Inderwildi and M. Kraft. Adsorption, Diffusion and Desorption of Chlorine on and from Rutile $TiO_2\{110\}$: A Theoretical Investigation. *ChemPhysChem*, 8:444–451, 2007. doi:10.1002/cphc.200600653.

[15] R. J. Kee, F. M. Rupley, and J. A. Miller. Chemkin-II: A fortran chemical kinetics package for the analysis of gas-phase chemical kinetics. Technical Report SAND89-8009, Sandia National Laboratories, 1989.

[16] S. J. Klippenstein, A. F. Wagner, R. C. Dunbar, D. M. Wardlaw, S. H. Robertson, and J. A. Miller. VariFlex. software package, 2002.

[17] A. Kobata, K. Kusakabe, and S. Morooka. Growth and transformation of $tio_2$ crystallites in aerosol reactor. *AIChE J.*, 37(3):347–359, 1991. doi:10.1002/aic.690370305.

[18] P. Koukkari and J. Niemela. Time-dependent reactor simulation by stationary state thermochemistry. *Comput. Chem. Eng.*, 21:245–253, 1997.

[19] F. A. Lindemann, S. Arrhenius, I. Langmuir, N. R. Dhar, J. Perrin, and W. C. M. Lewis. Discussion on "the radiation theory of chemical action". *Trans. Faraday Soc.*, 17:598–606, 1922. doi:10.1039/TF9221700598.

[20] J. A. Montgomery, Jr., M. J. Frisch, J. W. Ochterski, and G. A. Petersson. A complete basis set model chemistry. VII. use of the minimum population localization method. *J. Chem. Phys.*, 112(15):6532–6542, 2000. doi:10.1063/1.481224.

[21] NIST. Chemical Kinetics Database on the Web. Standard Reference Database 17, version 7.0 (web version), release 1.4, November 2007. URL http://kinetics.nist.gov/.

[22] R. Patterson, J. Singh, M. Balthasar, M. Kraft, and J. R. Norris. The linear process deferment algorithm: A new technique for solving population balance equations. *SIAM J. Sci. Comput.*, 28(1):303–320, 2006. doi:10.1137/040618953.

[23] R. I. A. Patterson and M. Kraft. Models for the aggregate structure of soot particles. *Combust. Flame*, 151:160–172, 2007. doi:10.1016/j.combustflame.2007.04.012.

[24] S. E. Pratsinis and P. T. Spicer. Competition between gas phase and surface oxidation of $TiCl_4$ during synthesis of $TiO_2$ particles- a two dimensional solution of the population balance equation. *Chem. Eng. Sci.*, 53:1861–1868, 1998. doi:10.1016/S0009-2509(98)00026-8.

[25] S. E. Pratsinis, H. Bai, P. Biswas, M. Frenklach, and S. V. R. Mastrangelo. Kinetics of titanium(IV) chloride oxidation. *J. Am. Ceram. Soc.*, 73:2158–2162, 1990.

[26] R. Raghavan. *Measurement of the High-Temperature Kinetics of Titanium Tetrachloride (TiCl4) Reactions in a Rapid Compression Machine*. PhD thesis, Case Western Reserve University, http://www.case.edu/cse/eche/people/students/theses/RaghavanRam-PhD.pdf, August 2001.

[27] J. Singh, R. I. A. Patterson, M. Balthasar, M. Kraft, and W. Wagner. Modelling soot particle size distribution: Dynamics of pressure regimes. Technical Report 25, c4e-Preprint Series, Cambridge, 2004.

[28] R. D. Smith, R. A. Bennett, and M. Bowker. Measurement of the surface-growth kinetics of reduced $TiO_2(110)$ during reoxidation using time-resolved scanning tunneling microscopy. *Phys. Rev. B: Condens. Matter Mater. Phys.*, 66(3):035409, Jul 2002. doi:10.1103/PhysRevB.66.035409.

[29] P. T. Spicer, O. Chaoul, S. Tsantilis, and S. E. Pratsinis. Titania formation by $TiCl_4$ gas phase oxidation, surface growth and coagulation. *J. Aerosol Sci.*, 33:17–34, 2002. doi:10.1016/S0021-8502(01)00069-6.

[30] N. Srinivasan, M.-C. Su, J. Michael, S. Klippenstein, and L. Harding. Reflected Shock Tube and Theoretical Studies of High-Temperature Rate Constants for OH + $CF_3H \leftrightharpoons CF_3$ + $H_2O$ and $CF_3$ + OH $\rightarrow$ Products. *J. Phys. Chem. A*, 111(29): 6822–6831, 2007. ISSN 1089–5639.

[31] S. Tsantilis and S. E. Pratsinis. Narrowing the size distribution of aerosol-made titania by surface growth and coagulation. *J. Aerosol. Sci.*, 35:405–420, 2004.

[32] R. H. West, G. J. O. Beran, W. H. Green, and M. Kraft. First-principles thermochemistry for the production of $TiO_2$ from $TiCl_4$. *J. Phys. Chem. A*, 111(18):3560–3565, 2007. doi:10.1021/jp0661950.

[33] R. H. West, M. S. Celnik, O. R. Inderwildi, M. Kraft, G. J. O. Beran, and W. H. Green. Toward a Comprehensive Model of the Synthesis of $TiO_2$ Particles from $TiCl_4$. *Ind. Eng. Chem. Res.*, 46(19):6147–6156, 2007. ISSN 0888-5885. doi:10.1021/ie0706414.

[34] Y. Xiong and S. E. Pratsinis. Formation of agglomerate particles by coagulation and sintering–part i. a two-dimensional solution of the population balance equation. *J. Aerosol Sci.*, 24(3):283–300, May 1993. doi:10.1016/0021-8502(93)90003-R.

[35] J. D. Yoon, K. Y. Park, and H. D. Jang. Comparison of titania particles between oxidation of titanium tetrachloride and thermal decomposition of titanium tetraisopropoxide. *Aerosol Sci. Technol.*, 37(8):621–627, 2003. doi:10.1080/02786820300907.